applied sciences

MDPI

Article

Bonding to Psychedelics: Synthesis of Molecularly Imprinted Polymers Targeting 4-Bromo-2,5-dimethoxyphenethylamine (2C-B)

Daniel Martins [1], Carlos Fernandes [1], Ricardo F. Mendes [2], Fernando Cagide [1], António Fernando Silva [1], Fernanda Borges [1] and Jorge Garrido [3,*]

[1] CIQUP-IMS, Department of Chemistry and Biochemistry, Faculty of Sciences, University of Porto, Rua do Campo Alegre s/n, 4169-007 Porto, Portugal; danieljosemmartins@gmail.com (D.M.); cevinhas@gmail.com (C.F.); fernando.fagin@fc.up.pt (F.C.); afssilva@fc.up.pt (A.F.S.); fborges@fc.up.pt (F.B.)
[2] CICECO-Aveiro Institute of Materials, Department of Chemistry, University of Aveiro, 3810-193 Aveiro, Portugal; rfmendes@ua.pt
[3] CIQUP-IMS, ISEP, Polytechnic of Porto, Rua Dr. António Bernardino de Almeida, 431, 4249-015 Porto, Portugal
* Correspondence: jjg@isep.ipp.pt

Abstract: The increasing interest in utilizing psychedelics for therapeutic purposes demands the development of tools capable of efficiently monitoring and accurately identifying these substances, thereby supporting medical interventions. 4-Bromo-2,5-dimethoxyphenethylamine (2C-B) has gained significant popularity as one of the most widely used psychedelic compounds in non-medical settings. In this study, we aimed to create a material with selective recognition of 2C-B by synthesizing a series of molecularly imprinted polymers (MIP) using 2C-B as the template and varying ratios of methacrylic acid (MAA) as the functional monomer (1:2, 1:3, and 1:4). Both thermal and microwave-assisted polymerization processes were employed. The molar ratio between the template molecule (2C-B) and functional monomer (MAA) was 1:4, utilizing a microwave-assisted polymerization process. Isotherm studies revealed a Langmuir's maximum absorption capacity (Bmax) value of 115.6 μmol·mg^{-1} and Kd values of 26.7 μM for this material. An imprint factor of 4.2 was determined for this material, against the corresponding non-imprinted polymer. The good selectivity against 14 other new psychoactive substances highlighted the material's potential for applications requiring selective recognition. These findings can contribute to the development of tailored materials for the detection and analysis of 2C-B, supporting advancements in non-medical use monitoring and potential therapeutic models involving psychedelics.

Keywords: psychedelic drugs; 2C-B; molecularly-imprinted polymer; microwave-assisted synthesis; selectivity

Citation: Martins, D.; Fernandes, C.; Mendes, R.F.; Cagide, F.; Silva, A.F.; Borges, F.; Garrido, J. Bonding to Psychedelics: Synthesis of Molecularly Imprinted Polymers Targeting 4-Bromo-2,5-dimethoxyphenethylamine (2C-B). *Appl. Sci.* **2024**, *14*, 1377. https://doi.org/10.3390/app14041377

Academic Editor: Jordi Puiggali

Received: 29 December 2023
Revised: 2 February 2024
Accepted: 5 February 2024
Published: 7 February 2024

1. Introduction

New psychoactive substances (NPS) constitute a heterogeneous group of chemical compounds meticulously formulated to emulate or elicit effects akin to conventional illicit drugs, frequently exploiting legal loopholes [1]. Within the realm of NPS, certain compounds, commonly referred to as psychedelics, possess the remarkable ability to instigate profound modifications in sensory perception, mood, emotion, cognition, and consciousness [2]. Psychedelics have been used for ceremonial, medicinal, and recreational purposes for millennia and a recent study estimated that 5.5 million people use psychedelic drugs annually in the United States of America [3]. Besides its widespread recreational use, recent promising results in the treatment of psychiatric disorders through psychedelic-assisted therapy has renewed the interest in the medical application of these compounds [2].

4-Bromo-2,5-dimethoxyphenethylamine (2C-B, Figure 1), a psychoactive analogue of mescaline, is currently one of the most popular psychedelics in non-medical contexts. After Shulgin et al. [4] first reported the synthesis and psychoactive effects of 2C-B, this substance

remained unnoticed in the public domain until it caught the attention of young people attending raves during early 1990s. Currently, 2C-B is the psychedelic drug most prevalent in Europe after LSD [5]. The circulation of drugs in unregulated markets increases the risks for people that use drugs and the challenges for forensic toxicologists, epidemiologists, or emergency doctors [6]. Thus, the development of tools that allow efficient monitoring and accurate identification and that support medical intervention related to psychedelic drugs is considered of utmost relevance [5–7].

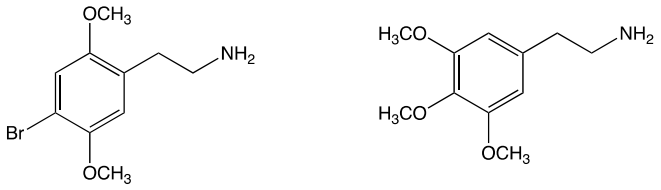

2C-B **Mescaline**

Figure 1. Chemical structures of 4-Bromo-2,5-dimethoxyphenethylamine (2C-B) and mescaline.

The development of analytical methods for specific analytes with a high degree of selectivity and sensitivity is often a challenging task for chemists and toxicologists due to the increased complexity of sample matrices. Molecular imprinting technology has gained prominence and it has been extensively utilized for important target compounds as antibodies receptors in diverse complex matrices. Inspired by antibody and enzyme mechanisms, molecularly imprinted polymers (MIP) were developed as a molecular recognition technology with a wide range of potential applications. MIP have been successfully applied in drug delivery [8], solid-phase extraction [9], catalysis [10], chromatographic or membrane-based separations [11,12], chemical sensing [13,14], and forensic chemistry [15].

A typical molecular imprinting process involves the formation of a pre-organized complex of a chosen template molecule (target molecule) and a functional monomer that either covalently links or non-covalently interacts with the template molecule followed by a crosslinking polymerization in the presence of an initiator and an appropriate crosslinker [16]. Non-covalent binding is much easier to achieve and is applicable to a wide range of targets, moreover, target binding and release are relatively fast [17]. One of the most significant and widely used non-covalent imprinting systems is the combination of methacrylic acid (MAA) as a functional monomer and ethylene glycol dimethacrylate (EGDMA) as a crosslinking agent in which MAA has the ability to form a hydrogen bond between varieties of template molecules [18]. Theorical studies pointed to MAA with chloroform as a porogen, as good options for the preparation of MIP targeting of phenethylamine-based drugs [19,20]. Polymerization is usually trigged by conventional heating, microwave (MW), photo-polymerization, and ultrasound [12]. Microwave has emerged as a green strategy in MIP synthesis, dramatically decreasing the time required in the polymerization process when compared to conventional heating [21]. Although the mechanism is still not well understood, the benefits of this clean technology are very clear, promoting homogeneous and rapid heat transfer through the reaction mixture, leading to higher reaction rates, short-term polymerization processes, and high yields [21]. After polymerization, the template molecule is removed, leaving behind binding cavities complementary in size, shape, and functional group assembly to the template molecule [16].

Herein we report the preparation of MIP targeting 2C-B through MW-assisted polymerization. Further optimization, such as best molar ratio template-monomer, optimal pH, or most efficient extraction solution composition was also explored. The capacity for selectively extracting the target compound from mixtures of new psychoactive substances, including *N*-benzylphenethylamine derivatives, was also evaluated. To the best of the authors' knowledge, this is the first time the preparation and study of MIPs targeting 2C-B is reported. This work is expected to expand the strategies available in biological

sample preparation and/or psychedelic drug analysis, considering its toxicological and forensic application.

2. Experimental

2.1. Chemicals, Instrumentation, and Chromatographic Conditions

2.1.1. Chemicals

Ethylene glycol dimethacrylate (EGDMA), methacrylic acid (MAA) and azobisisobutyronitrile (AINB) were purchased from Sigma Aldrich (St. Louis, MO, USA) or Alfa-Aesar (Haverhill, MA, USA). All other reagents and solvents were pro analysis grade and were acquired from Carlo Erba Reagents (SDS, Messia-sur-Sorne, France) and Scharlab (Barcelona, Spain) and were used without additional purification.

4-Bromo-2,5-dimethoxyphenethylamine (2C-B) and all psychoactive compounds tested in this study were prepared following synthetic procedures published by our group [22,23]. 2C-B was prepared by a straightforward synthetic route. Briefly, 2,5-dimethoxynitrostyrene was prepared through the condensation of 2,5-dimethoxybenzaldehyde and nitromethane. The obtained nitrostyrene was further reduced to phenethylamine with lithium aluminum hydride in anhydrous tetrahydrofuran. The addition of elemental bromine to a solution of the phenethylamine in acetic acid afforded the target compound, 4-bromo-2,5-dimethoxyphenethylamine.

All compounds were fully characterized by mass spectrometry (MS) and nuclear magnetic resonance (NMR). Citrate buffer (0.01 M, pH = 3), phosphate buffer (0.01 M, pH = 5 and pH = 7), and carbonate buffer (0.01 M, pH = 10) solutions were prepared according to the European Pharmacopoeia [24]. All aqueous solutions were prepared using ultra-pure water (Milli-Q-50 18 MΩ·cm).

2.1.2. Instrumentation

Compounds and polymers were weighted in an ABJ-NM/ABS-N balance (Kern, Ballingen, Germany). MW-assisted synthesis was performed in an Initiator Microwave Synthesizer (Biotage, Uppsala, Sweden). Thermal synthesis was performed in a Mya 4 Reaction Station (Radley, Essex, UK). Template removal was accomplished using an Isolera™ Prime (Biotage, Uppsala, Sweden), after packing prepared polymers into empty Biotage® SNAP 10 g cartridges, between fritted disks. Quantitative analysis was performed on a Shimadzu ultra-fast high-performance liquid chromatograph (uHPLC) LC-20AD Prominence Liquid Chromatograph (Shimadzu, Tokyo, Japan) with an SPD-M20A diode array detector (SPD-M20A). Separation was performed on a Luna C18-2 (Phenomenex, Torrance, CA, USA) column 150 mm × 4.6 mm, 5 µm. The chromatographic data was processed using the software package LabSolutions (Version 5.41 SP1, Shimadzu, Japan). Thermogravimetric analysis and differential thermal analysis were carried out using a Hitachi STA300 (Tokyo, Japan) thermogravimetric analyzer. The samples were heated from 30–900 °C under a nitrogen flow at 10 °C min^{-1}. Fourier Transform Infrared (FTIR) spectra were recorded using a Bruker Tensor 27 (resolution 2 cm^{-1}, 256 scans, Bruker, Billerica, MA, USA) in the spectral range of 4000–300 cm^{-1}.

2.1.3. Chromatographic Conditions

Chromatographic separation was carried out using a 26 min elution program with 0.2 M triethylammonium phosphate (TEAP) buffer adjusted to pH3 (mobile phase A) and 0.2 M TEAP buffer/ACN (30:70, mobile phase B), at a column temperature of 35 °C. A flow rate of 1 mL·min^{-1} was used in accordance with the following gradient: 20% mobile phase B for 0–10 min, increased to 45% for 8 min, slowly increased to 55% for 4 min more, sharply increased to 90% for 0.5 min, held for 1.5 min to clean residual polar compounds, and finally decreased to 20% in 0.5 min. Each compound was injected individually to study retention times and UV-spectra. Diode-array detection was set to collect data at 295 nm.

2.2. Polymer Preparation

MIP and non-imprinted polymers (NIPs) were prepared by bulk polymerization using different template-functional monomer molar ratios. Molar quantities are depicted in Table 1. Polymer monoliths were obtained through MW- and thermal-assisted synthesis.

Table 1. Molar equivalents of template and functional polymers in pre-polymerization solution.

Preparation Method	Polymer	Molar Ratio (Template: Functional Monomer)
MW	MIP1	1:2
	MIP2	1:3
	MIP3	1:4
Thermal	MIP4	1:2
	MIP5	1:3
	MIP6	1:4

2.2.1. Microwave-(MIP 1–3) and Thermal-Assisted (MIP 4–6) Synthesis

2C-B (free base) and MAA were dissolved in $CHCl_3$ in a microwave vial. The mixture was kept in the dark overnight to allow the self-assembly of template and monomer. EGDMA (20 eq.) and AINB (4 eq.) were then added, the mixture stirred for 5 min, purged with nitrogen, and sealed with a septum. The pre-polymerization mixture was then irradiated at 70 °C for 2 h with absorbance level set to high. The resulting polymer monolith was then carefully crushed in a mortar, rinsed with methanol, and dried overnight in a vacuum oven at 40 °C.

The same procedure described for MW-assisted synthesis was followed for MIP thermal-assisted synthesis. Polymerization was achieved through heating the vials with agitation in a reaction station Mya 4 for a duration of 24 h.

2.2.2. Template Removal

A mixture of methanol with acetic acid (10%, v/v) was forced to pass through synthesized polymers packed into empty Biotage® SNAP cartridges using the Biotage Isolera pump, at 1 mL·min^{-1} rate for a duration of 48 h. Finally, polymers were thoroughly washed with methanol (120 mL, 3 mL·min^{-1}) followed by phosphate buffer pH7 (120 mL, 3 mL·min^{-1}). The quantitative removal of template was confirmed by uHPLC analysis.

2.2.3. Non-Imprinted Polymers

The procedure to prepare MW- (NIP 1–3) and TH-assisted (NIP 4–6) non-imprinted polymers was similarly used in imprinted polymers, without adding the template molecule. The washing step was also applied.

2.3. Binding Batch Experiments

2.3.1. General Procedure

For each prepared MIP and NIP, 10 mg of polymer were weighed into a series of eppendorfs and 1 mL of loading solution (i.e., buffer solution containing variable amounts of 2C-B) was added. The eppendorfs were stoppered and equilibrated with agitation (400 rpm) at 25 °C during 24 h. After the removal of supernatant, the concentration of unbounded analyte in the solution, F (µM), was determined by uHPLC following the procedure described in Section 2.1. Blank assays were performed for each batch experiment. All experiments were performed in triplicate.

2.3.2. pH Study

The effect of pH on MIP binding was evaluated using different buffer solutions (pH = 3, 5, 7, and 10). The loading solution was prepared with the respective buffer solution and the polymer was incubated as described in the general procedure. The unbounded 2C-B (F) in

supernatant was determined by uHPLC and recovery, calculated as the ratio of unbound 2C-B (F) and the initial concentration of 2C-B (C_0).

2.3.3. Adsorption Equilibrium Time

To determine the required time for reaching equilibrium, a loading solution of 2C-B (0.67 mM) at pH 7, was added to 9 samples containing 10 mg of MIP. The incubation was interrupted at different times: 0, 0.2, 0.3, 0.5, 1.5, 6.0, 12.0, 15.0, and 24 h.

2.3.4. Effect of Extraction Solution Composition

To evaluate the optimal ratio of acetic acid in methanol extraction solution, analyte recovery was calculated using three different initial concentrations: 0.05, 0.25, and 0.50 mM. After a 12 h incubation, the loading solution was removed, the polymer was washed with phosphate buffer solution (pH = 7), and the analyte was extracted with five different extraction solutions containing 0, 5, 10, 15, and 20%, of acetic acid in MeOH (v/v).

2.4. Binding Parameters Determination and Isotherm Fitting Models

2.4.1. Binding Parameters

Binding parameters of polymers were determined using batch experiments with further isotherm studies [25]. Analyte solutions (0–2 mM) were freshly prepared for each set of experiments. Temperature was kept at 293 K. After reaching equilibrium, the concentration of free analyte, F (µM), was determined by uHPLC and analyte bounded to polymer, B (µmol·mg^{-1}), was calculated through the Equation (1):

$$B = \frac{(C_0 - F) \times V}{m_P} \quad (1)$$

where C_0 (µM) is the initial concentration of analyte solution, V (mL) is the volume of 2C-B solution, and m_P (mg) is the polymer mass used in each experiment.

2.4.2. Isotherm Fitting Models

The plotting of B versus F yields a binding isotherm, making possible to determine apparent parameters through fitting. Adsorption isotherm models evaluated through non-linear fitting were as follows:

$$\text{Langmuir } B = \frac{F \times B_{max}}{Kd + F} \quad (2)$$

$$\text{Freundlich } B = A \times F^m \quad (3)$$

In Equation (2), B_{max} and Kd are the density of binding sites and the dissociation constant of these sites, respectively. The Langmuir model considers all binding sites are equivalent. When $F = Kd$, then $B = 0.5 \times Bmax$. Kd can be defined as the concentration of free template at which 50% of imprinted sites are occupied, and $Bmax$ as the value of B when all of the binding sites are occupied. In Freundlich model (Equation (3)), A and m are dimensionless constants that can be used to evaluate the binding site heterogeneity and determine dissociation constants and binding site densities [26]. The best fit was assessed by Akaike's method and presented as the "probability of correct model" [27].

2.4.3. Imprinting and Selectivity Factors

In each experiment the total number of moles of analyte, n_{total}, is described as:

$$n_{total} = n_{free} + n_{bound} \quad (4)$$

where n_{free} and n_{bound} represent the number of free and bound analyte, respectively. Equation (4) allows the definition of the line of analyte conservation, constructed by the y-

interception point if considering that all analyte is bonded (F = 0, limit value of B), and by x-interception point if all analyte is free (B = 0, limit value of F).

$$D = \frac{B}{F} = \frac{n_{bound/m_P}}{n_{free/V}} \quad (5)$$

The distribution factor (D) was calculated with Equation (5) through the (x,y) values (B and F, respectively) of the point of the intersection of the line of ligand conservation (C_0 = 1.0, 1.5 and 2.0 mM) with MIP and with NIP isotherm functions [28].

The imprinting factor (IF) was calculated by comparing the distribution factors of imprinted (D_{MIP}) and non-imprinted (D_{NIP}) polymers through Equation (6).

$$IF = \frac{D_{MIP}}{D_{NIP}} = \frac{n_{bound,MIP}/n_{free,MIP}}{n_{bound,NIP}/n_{free,NIP}} \quad (6)$$

Selectivity was studied by analyte batch-binding evaluation in the presence of 14 different competing compounds (C_0 = 0.35 mM for all competitors). The selectivity factor (S) was calculated using Equation (7) by comparing the MIP distribution factors of analyte ($D_{2C\text{-}B}$) and competitors ($D_{competitor}$):

$$S = \frac{D_{2C-B}}{D_{competitor}} \quad (7)$$

3. Results and Discussion

3.1. Synthesis and Template Removal

The use of appropriate molar ratios of template/functional monomer/cross-linker is very important to improve the specific affinity of the polymers and the number of recognition sites of the MIP. High ratios of functional monomer/template typically result in high non-specific affinity, while low ratios produce fewer complexation events due to insufficient functional groups [29]. The cross-linker molar amount used in each of the formulations prepared complied with the functional monomer to cross-linker molar ratio of 1:5 [29]. Molecularly imprinted and non-imprinted polymers were prepared through MW- (**1–3**) and thermal-assisted synthesis (**4–6**), using different imprinting ratios (1:2, 1:3, 1:4; template/functional monomer; Table 1), and its binding properties characterized.

The usage of microwave irradiation consistently reduces the polymerization time with respect to traditional heating. This is due to the promotion of high heat transfer into the reaction mixture that facilitated the increase in reaction rate and the decrease in the energy consumption [12]. The effect of irradiation on polymerization was assessed by visual inspection of obtained materials, through experiments with successive temperature increases starting at 55 °C up to 80 °C. The solution increased fluidity with extended times but only from 70 °C onwards a monolith was obtained after 2 h of irradiation. Comparing with thermal heating, the use of MW reduced the preparation time by 12-fold, using the same temperature. Template removal was achieved after washing with a mixture of methanol: acetic acid (9:1, 1 mL·min^{-1}, 48 h). Experiments using the same washing volume at higher flux (up to 10 mL·min^{-1}) and higher acetic acid content (up to 20% v/v) did not improve template removal times. Regarding the mass of polymer used in each experiment, the use of 10 and 30 mg of polymer in 1 mL of solution was evaluated and equivalent results were obtained.

3.2. Characterization

3.2.1. FTIR Characterization of MIPs and NIPs

The FTIR spectra of both MIPs and NIPs were obtained to investigate the backbone structure of the prepared polymers (Figure 2).

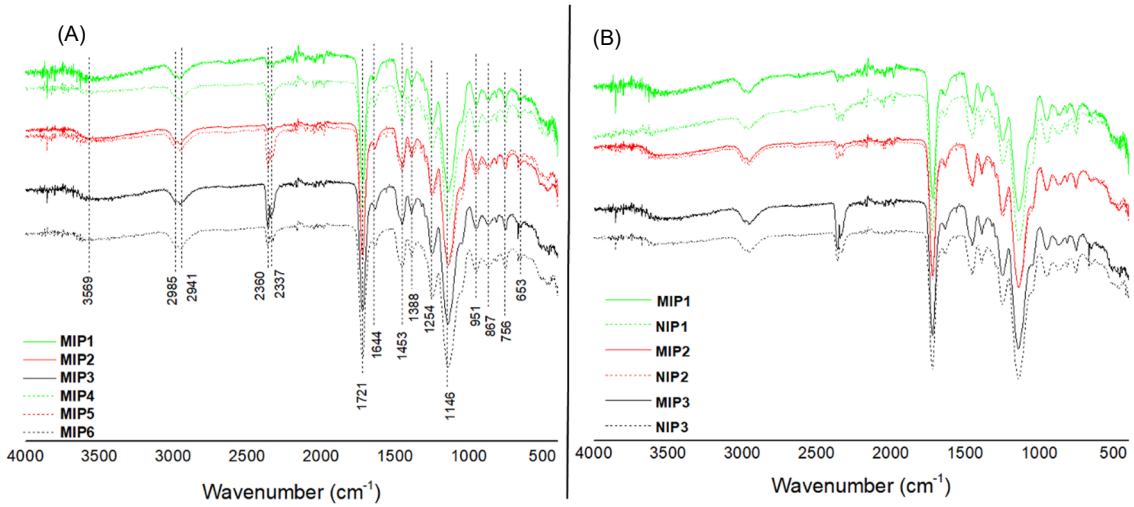

Figure 2. FTIR spectra of prepared MIPs using thermal and microwave-assisted polymerization (**A**) and comparison of the spectroscopy data between the MIP 1–3 and their related NIP 1–3 (**B**).

As the starting materials of the MIP and NIP, such as the functional monomer, cross-linker, initiator, etc., were the same, all FTIR spectra obtained are similar (Figure 2A). The O-H stretching peak at 3569 cm^{-1} and the O–H bending vibration at 1388 cm^{-1} confirm the presence of carboxylic acid groups. The absorption band at 2854 cm^{-1} corresponds to the asymmetrical vibration of C–H bond of the $–CH_2$ polymer chain. The presence of two significant peaks at 1721 and 1146 cm^{-1} is related to C=O and C–O–C stretching vibration, respectively, and shows the existence of EGDMA cross-linker [30]. The $–CH_3$, $–CH_2$ deformation vibrations spectra are clearly detected at 1453 cm^{-1} [31]. The absence of the MAA and EGDMA C=C double bond stretching at 1644 cm^{-1} in MIPs and NIPs indicates that the polymerization process was successful [31].

Thermogravimetric Analysis

The thermal behavior of MIPs was evaluated by measuring the weight loss (TGA, Figure 3A) and the rate of weight loss (DTG, Figure 3B) after heating the sample at a constant rate.

The obtained thermograms were similar for all MIPs prepared, presenting mainly three steps of weight loss by analysis of both TG and DTG thermograms. All of the MIPs lose water in the initial step, up to approximately 100 °C. After that, a second step was observed between 250 °C and 370 °C, which was due to the depolymerization of Poly(MAA) resulting in a small yield of monomer [31]. The third major step is initiated at ~370 °C due to an elimination of the water molecule adsorbed between pairs of carboxylic groups [31]. A more detailed analysis of thermograms in the 425–525 °C range, suggested that MIPs with a higher ratio of template and functional monomer led to a higher amount of weight loss. Since a lower amount of template was used in both MIP 3 and MIP 6, the content of polymer backbone is higher per unit of mass of MIPs when compared with those prepared with higher quantities of 2C-B.

The peaks assigned in DTG showed the inflection point of the TG thermograms, which allowed us to conclude the difference between materials prepared by their stability. By comparing the weight loss rate of the MIPs and NIPs prepared through MW-assisted synthesis, it was possible to verify that for the same template:functional monomer ratio used, the peaks appeared at similar temperatures. However, when comparing materials with different ratios, a shift of temperatures is observed for both MIP1 and NIP1, which could be due to a lower polymer backbone content, leading to a poor thermal stability.

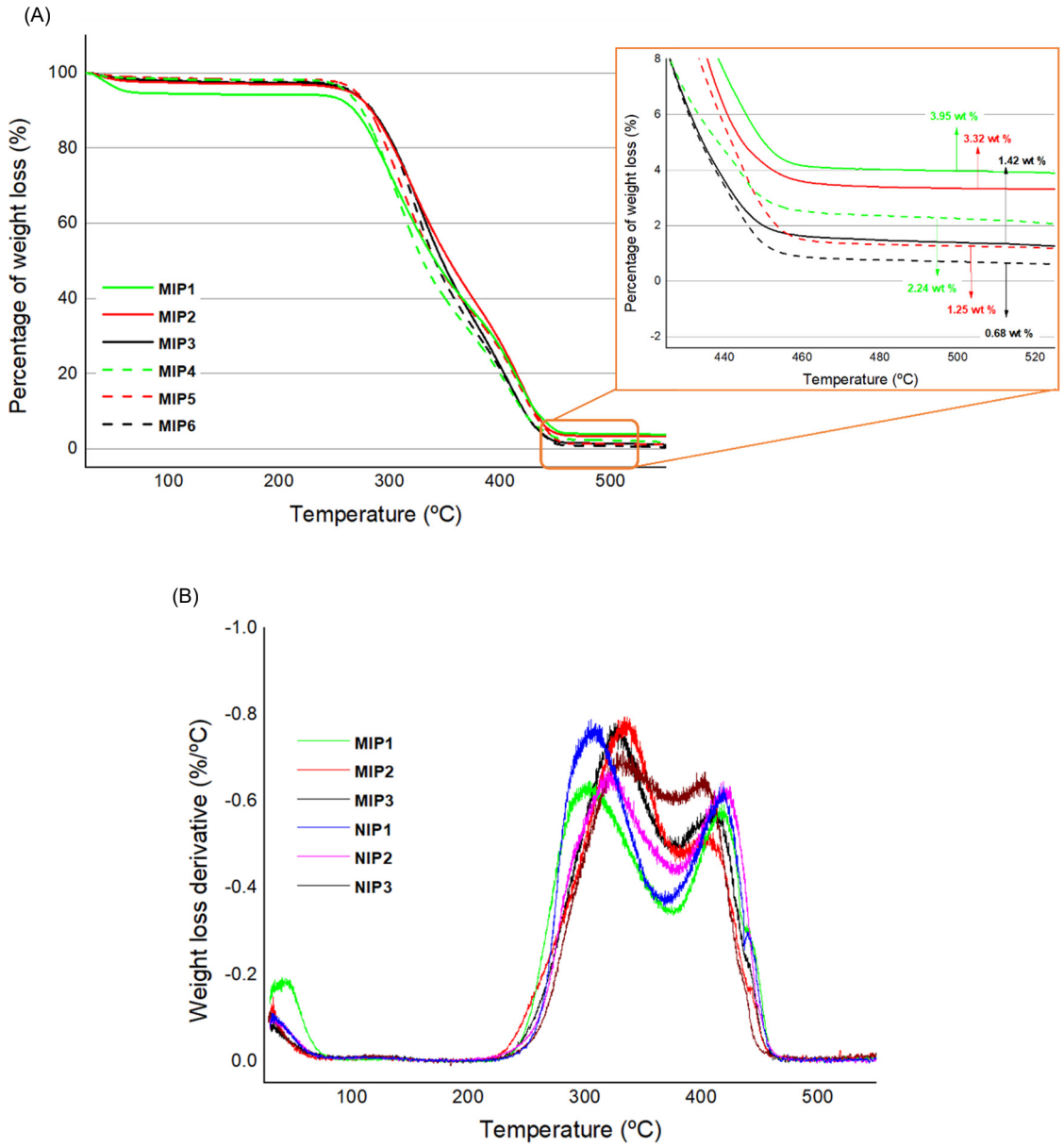

Figure 3. Thermoanalysis curves of prepared materials: (**A**) thermogravimetric (TG) analysis and (**B**) derivative of thermogravimetric analysis (DTG).

3.3. Binding Optimization

Optimization of binding conditions was assessed through the study of the required time to reach equilibrium (Figure 4) and the concentration of acetic acid in methanol (Figure 5) for extraction procedure. At least 3 h were required for *B* values to reach the equilibrium. This feature can restrict the application of the material to lower concentrations. Maximum recovery is achieved with 10% acetic acid, further increases did not improve extraction.

The influence of pH on binding was evaluated over the range 3 to 10. As 2C-B is a weak base (pKa = 9.8) and MAA a weak acid (pKa = 4.7), the pH of the solution can influence template-polymer interaction since it will determine which chemical species are present in solution. The data found (Figure 6) showed that higher recovery was obtained between the pKa of 2C-B and MAA (5 < pH < 10). This pH effect can possibly be explained by increased adsorption promoted by ionic interaction, which will be higher with the protonated amine group of 2C-B and anionic carboxylate groups of MAA. Therefore, in the subsequent experiments pH was adjusted to pH = 7.

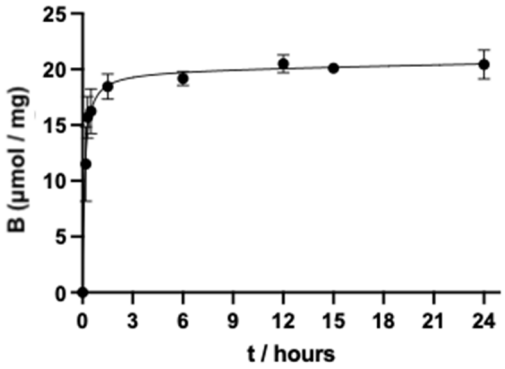

Figure 4. Kinetics of adsorption of 0.17 mM of 2C-B in phosphate buffer (pH = 7) using 10 mg of MIP 3.

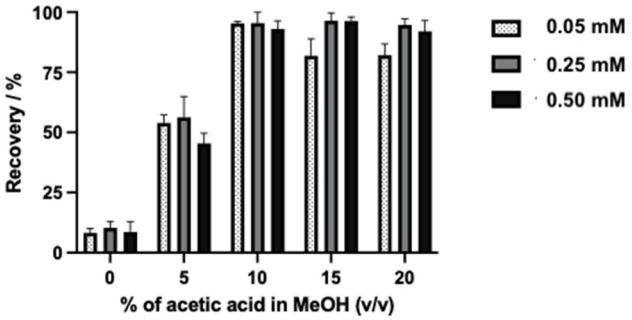

Figure 5. Rate of recovery of bonded compound after washing loaded MIP with methanol containing 0–20% (*v*/*v*) of acetic acid.

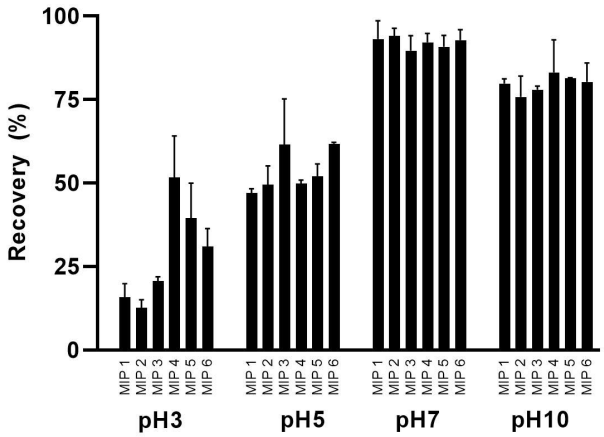

Figure 6. Effect of pH on average recovery (mean ± SD, *n* = 2) of 2C-B (0.35 mM) after incubation with molecularly imprinted polymers.

Binding Parameters and Isotherm Fitting

For all studied MIP, B *versus* F isotherm plots of equilibrium batch binding experiments (Figure 7) exhibit a saturation-type curve. This supports the current understanding that adsorption at MIP occurs via a mixture of specific binding, due to the presence of specific cavities, with non-specific binding, related to surface adsorption by Van der Waals forces [25]. NIP isotherm plots showed a lower saturation progress when compared with the corresponding MIP.

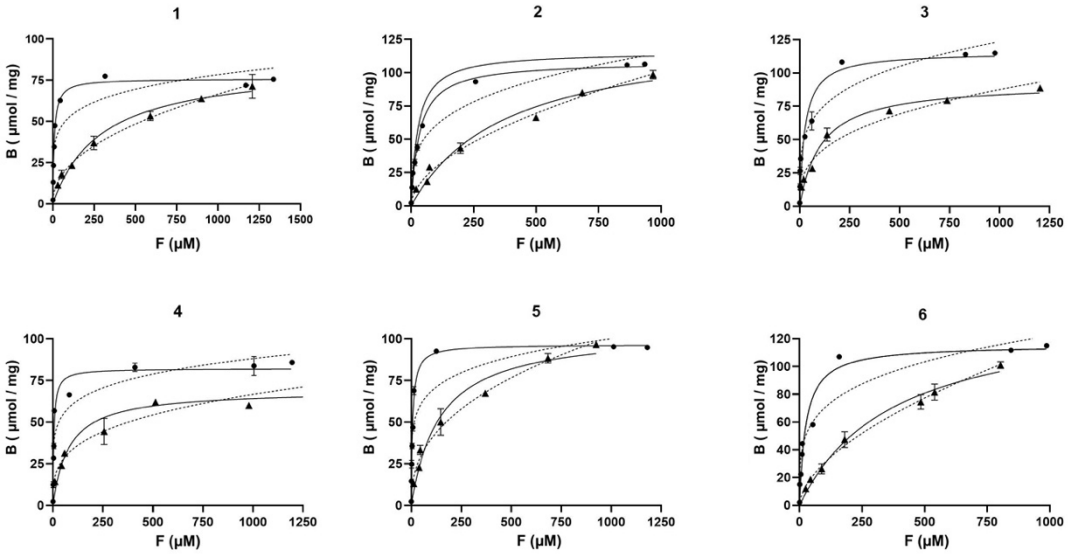

Figure 7. Equilibrium binding isotherms for 2C-B incubated in MIP 1–6 (●) and NIP 1–6 (▲) at 25 °C. Non-linear fitting using Langmuir (—) and Freundlich (···) models are pictured. Data represents mean ± SD, n = 3.

Strategies to compare imprinted and non-imprinted polymers and evaluate their performance have been a source of debate [25,32]. Theoretical isotherm models have been extensively utilized to conduct comparative analyses of materials [25]. These models provide a means for quantitative analysis, although it should be noted that the resulting values are considered apparent. Distribution factors D, when calculated by the x,y-interception points of isotherms (see experimental section), allow further comparison with non-imprinted material (i.e., imprinting factor IF) or competitor molecules (i.e., selectivity factor S).

Non-linear fitting of Langmuir and Freundlich isotherm models (Equations (2) and (3), respectively) were tested. The Langmuir model assumes that adsorption follows a homogeneous monolayer coverage. It considers a finite number of binding sites such that once these sites are filled no further molecules can bond. On the other hand, Freundlich represents a reversible reaction where multilayer adsorption is permitted. In general, in our batch experiments, the Langmuir model afforded the best fitting from the analysis of parameters, with a lower sum of squares (SS), higher correlation coefficients (R^2), and overall higher probability of being the correct model using Akaike's method, when compared with Freundlich model (Table 2). Other adsorption models that consider a heterogeneous distribution of binding sites, namely bi-Langmuir, were also tested but the fitting did not meet requirements.

MIP obtained *via* MW-assisted synthesis (MIP 1–3) showed Langmuir's *Bmax* values ranging from 75.9 to 115.6 µmol·mg^{-1} and *Kd* values ranging from 8.6 to 32.8 µM (Table 2). The imprinted polymers prepared via thermal heating show *Bmax* values in the range of 82.9–115.4 µmol·mg^{-1} and *Kd* values ranging from 4.9 to 25.6 µM (Table 2). The exhibition of specific and non-specific binding behavior and equivalent *Bmax* and *Kd* in MW- and TH-assisted polymerization can be an indication that apparently radiation did not affect the formation of cavities with complementary features. Considering the variation in template-functional monomer molar ratio, there is, in general, an increase in *Bmax* from a molar ratio of 1:2 to 1:4 in both preparation systems. MIP 3 and 6 present the higher values (115.6 ± 5.5) µmol·mg^{-1} and (115.4 ± 4.5) µmol·mg^{-1}, respectively.

To examine the impact of the non-selective interactions of the analyte and polymer on the *Kd* and *Bmax* descriptor values, the binding differential was examined through *IF*. For the ease of polymer comparison, *IF* values were determined using the line of ligand conservation method (see Section 2). Data revealed that the six prepared polymers follow the same *IF* decaying values, in the range of 1.0–2.0 mM (Figure 8). In general, MIP

distribution factor *D* falls (Equation (5)), while in the NIP isotherm curve the curvature is less pronounced, which could be explained by the lack of specific binding, promoting less variation in the middle range of studied *F* concentrations. This data provides information on at which concentrations the MIP can be more efficient than its non-imprinted pair.

Table 2. Non-linear fitting parameters (mean ± SD, n = 2) through Langmuir and Freundlich isotherm models.

	Langmuir					**Freundlich**				
	Isotherm Parameters		**Fitting Parameters**			**Isotherm Parameters**		**Fitting Parameters**		
	B_{max}	*Kd*	R^2	*SS*	*P(AIC)*	*A*	*m*	R^2	*SS*	*P(AIC)*
MIP 1	(75.9 ± 1.6)	(8.6 ± 0.8)	0.9797	266	>99.9	(23.8 ± 3.6)	(0.17 ± 0.03)	0.8146	2426	<0.01
MIP 2	(108.3 ± 1.6)	(32.8 ± 2.0)	0.9932	138	>99.9	(16.9 ± 0.3)	(0.02 ± 0.02)	0.9443	1421	<0.01
MIP 3	(115.6 ± 5.5)	(26.7 ± 6.2)	0.9695	2031	8.8	(24.3 ± 2.9)	(0.24 ± 0.02)	0.9829	1566	91.2
MIP 4	(82.9 ± 2.2)	(4.9 ± 0.6)	0.9658	562	>99.9	(29.2 ± 3.4)	(0.16 ± 0.02)	0.9005	1632	<0.01
MIP 5	(96.6 ± 1.4)	(6.8 ± 0.4)	0.9921	167	>99.9	(32.2± 4.2)	(0.16 ± 0.02)	0.8594	2966	<0.01
MIP 6	(115.4 ± 4.5)	(25.6 ± 4.4)	0.9556	1367	99.1	(23.1 ± 3.4)	(0.24 ± 0.02)	0.9255	2294	0.9

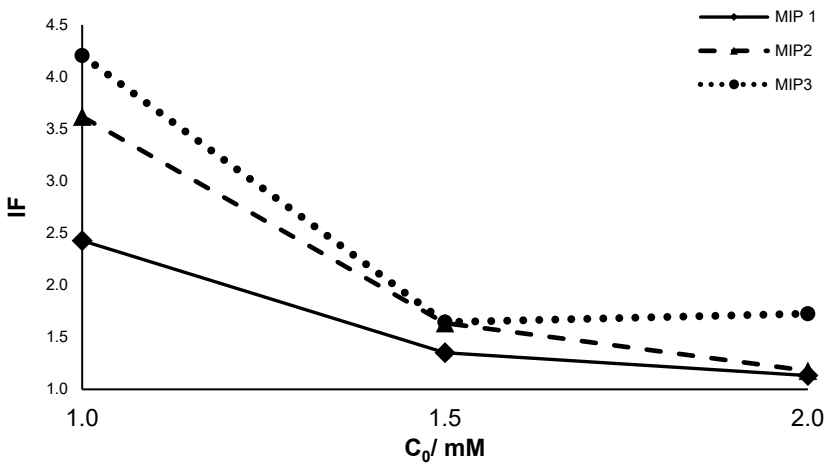

Figure 8. Imprinting factor of three MW-assisted MIP/NIP preparations.

The selectivity of MIPs depends on their ability to maintain the fidelity of the binding sites formed by template imprinting. Molecular selectivity was established from investigations conducted under competitive batch binding conditions with 2C-B analogues and other common NPS, using MIP 3 (Figure 9). Selectivity was higher for ketamine and lower for compounds chemically similar to 2C-B, such as 2C-I and 2C-C.

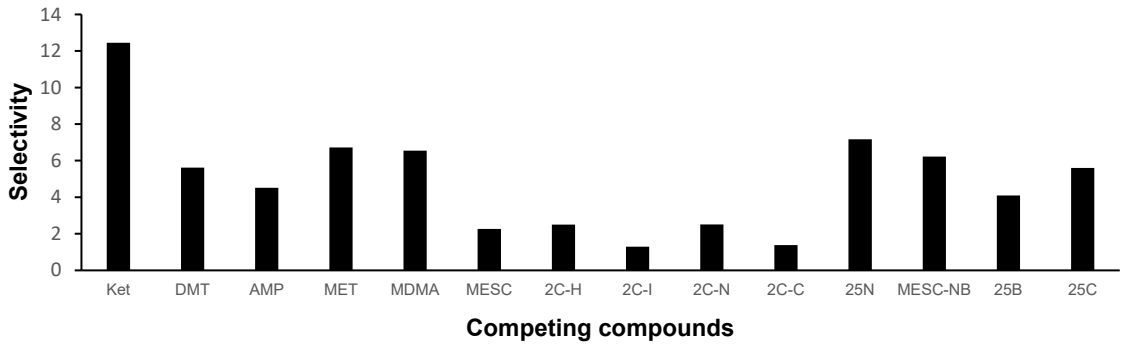

Figure 9. Selectivity factor of MIP 3 towards different similar structures. KET: Ketamine; DMT: dimethyltryptamine; AMP: amphetamine; MET: methamphetamine; MDMA: 3,4-methylenedioxym-

etamphetamine; MESC: 3,4,5-trimethoxyphenethylamine, mescaline; 2C-H: 2,5-dimethoxyphenethylamine; 2C-I: 2,5-dimethoxy-4-iodophenethylamine; 2C-N: 2,5-dimethoxy-4-nitrophenethylamine; 2C-C: 4-chloro-2,5-dimethoxyphenethylamine; 25N: *N*-2-methoxybenzyl-2,5-dimethoxy-4-nitrophenethylamine; MESC-NB: *N*-2-methoxybenzyl-3,4,5-trimethoxyphenethylamine; 25B: *N*-2-methoxybenzyl-4-bromo-2,5-dimethoxy-phenethylamine; 25C: *N*-2-methoxybenzyl-4-chloro-2,5-dimethoxy-phenethylamine.

The study of selectivity included also the forensic relevant NBOMes (*N*-2-methoxybenzyl-dimethoxy-phenethylamine derivatives; 25B and 25C). Reports of severe clinical toxicity and deaths have been associated with intentional and unintentional (e.g., sold on the internet allegedly as 2C-B [33]) containing NBOMe derivatives [34]. For these potent *N*-benzylated derivatives, good selectivity values were achieved, with a five times lower *D* value.

4. Conclusions

In this study, we employed 2C-B as a template molecule and methacrylic acid as a functional monomer, comparing two polymerization methods: thermal and microwave-assisted. The outcome was the successful synthesis of molecularly imprinted polymers (MIPs) with high recognition for 2C-B and good selectivity on a wide range of new psychoactive substances. Our analysis, conducted using the Langmuir model, revealed that both polymerization methods demonstrated a striking similarity. However, the microwave-assisted approach demonstrated an additional advantage—its environmentally friendly and expedited nature, highlighting its potential as a greener and more efficient process.

This study not only adds to our understanding of molecularly imprinted polymers but also paves the way for further investigations into the recognition of psychedelics using this approach. By shedding light on the compatibility of diverse molecules with MIPs, our work offers a foundation for future explorations in this captivating field.

Author Contributions: Conceptualization, A.F.S., D.M., F.B. and J.G.; Methodology, D.M., C.F., R.F.M., F.C. and F.B.; Investigation, D.M., C.F., R.F.M. and F.C.; Writing—original draft, D.M. and C.F.; Writing—review & editing, D.M., C.F. and J.G.; Supervision, A.F.S. and F.B.; Funding acquisition, F.B. All authors have read and agreed to the published version of the manuscript.

Funding: This work was funded by FEDER funds through the Operational Programme Competitiveness Factors-COMPETE and national funds from the FCT, Foundation for Science and Technology, under research grants (Grants UIDB/00081/2020 (CIQUP), LA/P/0056/2020 (IMS). The D. Martins (PD/BD/135122/2017) grant and FC, CF [CEECIND/00823/2021], contracts are supported by FCT and FEDER/COMPETE. This work was developed within the scope of the project CICECO-Aveiro Institute of Materials, UIDB/50011/2020, UIDP/50011/2020, and LA/P/0006/2020, financed by national funds through the FCT/MCTES (PIDDAC). RM gratefully acknowledges FCT for a Junior Research Position (CEECIND/00553/2017).

Institutional Review Board Statement: Not applicable.

Informed Consent Statement: Not applicable.

Data Availability Statement: Data are contained within the article.

Conflicts of Interest: The authors declare no conflict of interest.

References

1. Shafi, A.; Berry, A.J.; Sumnall, H.; Wood, D.M.; Tracy, D.K. New psychoactive substances: A review and updates. *Ther. Adv. Psychopharmacol.* **2020**, *10*, 2045125320967197. [CrossRef]
2. Vargas, M.V.; Meyer, R.; Avanes, A.A.; Rus, M.; Olson, D.E. Psychedelics and Other Psychoplastogens for Treating Mental Illness. *Front. Psychiatry* **2021**, *12*, 727117. [CrossRef]
3. Livne, O.; Shmulewitz, D.; Walsh, C.; Hasin, D.S. Adolescent and adult time trends in US hallucinogen use, 2002–2019: Any use, and use of ecstasy, LSD and PCP. *Addiction* **2022**, *117*, 3099–3109. [CrossRef]
4. Shulgin, A.T.; Carter, M.F. Centrally active phenethylamines. *Psychopharmacol. Commun.* **1975**, *1*, 93–98.

5. Hirschfeld, T.; Smit-Rigter, L.; van der Gouwe, D.; Reiche, S.; Stöver, H.; Majić, T. Safer Tripping: Serotonergic Psychedelics and Drug Checking. Submission and Detection Rates, Potential Harms, and Challenges for Drug Analysis. *Curr. Addict. Rep.* **2021**, *8*, 389–398. [CrossRef]
6. Nutt, D. New psychoactive substances: Pharmacology influencing UK practice, policy and the law. *Br. J. Clin. Pharmacol.* **2020**, *86*, 445–451. [CrossRef] [PubMed]
7. Zawilska, J.B.; Kacela, M.; Adamowicz, P. NBOMes-Highly Potent and Toxic Alternatives of LSD. *Front. Neurosci.* **2020**, *14*, 78. [CrossRef] [PubMed]
8. Lusina, A.; Cegłowski, M. Molecularly Imprinted Polymers as State-of-the-Art Drug Carriers in Hydrogel Transdermal Drug Delivery Applications. *Polymers* **2022**, *14*, 640. [CrossRef] [PubMed]
9. Hu, T.; Chen, R.; Wang, Q.; He, C.; Liu, S. Recent advances and applications of molecularly imprinted polymers in solid-phase extraction for real sample analysis. *J. Sep. Sci.* **2021**, *44*, 274–309. [CrossRef] [PubMed]
10. Muratsugu, S.; Shirai, S.; Tada, M. Recent progress in molecularly imprinted approach for catalysis. *Tetrahedron Lett.* **2020**, *61*, 151603. [CrossRef]
11. Gao, M.; Gao, Y.; Chen, G.; Huang, X.; Xu, X.; Lv, J.; Wang, J.; Xu, D.; Liu, G. Recent Advances and Future Trends in the Detection of Contaminants by Molecularly Imprinted Polymers in Food Samples. *Front. Chem.* **2020**, *8*, 616326. [CrossRef]
12. Donato, L.; Nasser, I.I.; Majdoub, M.; Drioli, E. Green Chemistry and Molecularly Imprinted Membranes. *Membranes* **2022**, *12*, 472. [CrossRef] [PubMed]
13. Dickert, F.L.; Thierer, S. Molecularly imprinted polymers for optochemical sensors. *Adv. Mater.* **1996**, *8*, 987–990. [CrossRef]
14. Kadhem, A.J.; Gentile, G.J.; Fidalgo de Cortalezzi, M.M. Molecularly Imprinted Polymers (MIPs) in Sensors for Environmental and Biomedical Applications: A Review. *Molecules* **2021**, *26*, 6233. [CrossRef] [PubMed]
15. Ferreira, J.B.; de Jesus Macrino, C.; Dinali, L.A.F.; Filho, J.F.A.; Silva, C.F.; Borges, K.B.; Romão, W. Molecularly imprinted polymers as a selective sorbent for forensic applications in biological samples—A review. *Anal. Bioanal. Chem.* **2021**, *413*, 6013–6036. [CrossRef] [PubMed]
16. Takeuchi, T.; Sunayama, H. Molecularly Imprinted Polymers. In *Encyclopedia of Polymeric Nanomaterials*; Kobayashi, S., Müllen, K., Eds.; Springer: Berlin/Heidelberg, Germany, 2021; pp. 1–5.
17. Mostafa, A.M.; Barton, S.J.; Wren, S.P.; Barker, J. Review on molecularly imprinted polymers with a focus on their application to the analysis of protein biomarkers. *TrAC Trends Anal. Chem.* **2021**, *144*, 116431. [CrossRef]
18. Shah, N.; Ul-Islam, M.; Haneef, M.; Park, J.K. A brief overview of molecularly imprinted polymers: From basics to applications. *J. Pharm. Res.* **2012**, *5*, e3317.
19. Ahmadi, F.; Ahmadi, J.; Rahimi-Nasrabadi, M. Computational approaches to design a molecular imprinted polymer for high selective extraction of 3,4-methylenedioxymethamphetamine from plasma. *J. Chromatogr. A* **2011**, *1218*, 7739–7747. [CrossRef]
20. Sales, T.A.; Ramalho, T.C. Computational design of synthetic receptors for drug detection: Interaction between molecularly imprinted polymers and MDMA (3,4-methylenedioxymethamphetamine). *Theor. Chem. Acc.* **2020**, *139*, 31. [CrossRef]
21. Viveiros, R.; Rebocho, S.; Casimiro, T. Green Strategies for Molecularly Imprinted Polymer Development. *Polymers* **2018**, *10*, 306. [CrossRef]
22. Martins, D.; Gil-Martins, E.; Cagide, F.; da Fonseca, C.; Benfeito, S.; Fernandes, C.; Chavarria, D.; Remião, F.; Silva, R.; Borges, F. Unraveling the In Vitro Toxicity Profile of Psychedelic 2C Phenethylamines and Their N-Benzylphenethylamine (NBOMe) Analogues. *Pharmaceuticals* **2023**, *16*, 1158. [CrossRef]
23. Martins, D.; Garrido, E.M.P.J.; Borges, F.; Garrido, J.M.P.J. Voltammetric profiling of new psychoactive substances: Piperazine derivatives. *J. Electroanal. Chem.* **2021**, *883*, 115054. [CrossRef]
24. Nahler, G. European Pharmacopoeia (Eur Ph). In *Dictionary of Pharmaceutical Medicine*; Nahler, G., Ed.; Springer: Vienna, Austria, 2009; p. 69.
25. Ansell, R.J. Characterization of the Binding Properties of Molecularly Imprinted Polymers. In *Molecularly Imprinted Polymers in Biotechnology*; Mattiasson, B., Ye, L., Eds.; Springer International Publishing: Cham, Switzerland, 2015; pp. 51–93.
26. Rampey, A.M.; Umpleby, R.J.; Rushton, G.T.; Iseman, J.C.; Shah, R.N.; Shimizu, K.D. Characterization of the Imprint Effect and the Influence of Imprinting Conditions on Affinity, Capacity, and Heterogeneity in Molecularly Imprinted Polymers Using the Freundlich Isotherm-Affinity Distribution Analysis. *Anal. Chem.* **2004**, *76*, 1123–1133. [CrossRef] [PubMed]
27. Arnold, T.W. Uninformative Parameters and Model Selection Using Akaike's Information Criterion. *J. Wildl. Manag.* **2010**, *74*, 1175–1178. [CrossRef]
28. Castell, O.K.; Barrow, D.A.; Kamarudin, A.R.; Allender, C.J. Current practices for describing the performance of molecularly imprinted polymers can be misleading and may be hampering the development of the field. *J. Mol. Recognit.* **2011**, *24*, 1115–1122. [CrossRef]
29. Barros, L.A.; Custodio, R.; Rath, S. Design of a new molecularly imprinted polymer selective for hydrochlorothiazide based on theoretical predictions using Gibbs free energy. *J. Braz. Chem. Soc.* **2016**, *27*, 2300–2311. [CrossRef]
30. Shaipulizan, N.S.; Md Jamil, S.N.A.; Kamaruzaman, S.; Subri, N.N.S.; Adeyi, A.A.; Abdullah, A.H.; Abdullah, L.C. Preparation of Ethylene Glycol Dimethacrylate (EGDMA)-Based Terpolymer as Potential Sorbents for Pharmaceuticals Adsorption. *Polymers* **2020**, *12*, 423. [CrossRef]
31. Pardeshi, P.M.; Mungray, A.A. Photo-polymerization as a new approach to fabricate the active layer of forward osmosis membrane. *Sci. Rep.* **2019**, *9*, 1937. [CrossRef]

32. Tóth, B.; Pap, T.; Horvath, V.; Horvai, G. Which molecularly imprinted polymer is better? *Anal. Chim. Acta* **2007**, *591*, 17–21. [CrossRef] [PubMed]
33. Hill, S.L.; Doris, T.; Gurung, S.; Katebe, S.; Lomas, A.; Dunn, M.; Blain, P.; Thomas, S.H.L. Severe clinical toxicity associated with analytically confirmed recreational use of 25I-NBOMe: Case series. *Clin. Toxicol.* **2013**, *51*, 487–492. [CrossRef]
34. Halberstadt, A.L. Pharmacology and Toxicology of N-Benzylphenethylamine ("NBOMe") Hallucinogens. In *Neuropharmacology of New Psychoactive Substances (NPS): The Science Behind the Headlines*; Baumann, M.H., Glennon, R.A., Wiley, J.L., Eds.; Springer International Publishing: Cham, Switzerland, 2017; pp. 283–311.